Available online at www.sciencedirect.com
SCIENCE DIRECT
Journal of Magnetic Resonance 178 (2006) 228–236
JMR Journal of Magnetic Resonance
www.elsevier.com/locate/jmr

Separation of ^{47}Ti and ^{49}Ti solid-state NMR lineshapes by static QCPMG experiments at multiple fields

Flemming H. Larsen [a,*], Ian Farnan [b], Andrew S. Lipton [c]

[a] Department of Food Science, Quality and Technology, The Royal Veterinary and Agricultural University, Rolighedsvej 30, DK-1958 Frederiksberg C, Denmark
[b] Department of Earth Sciences, University of Cambridge, Cambridge CB2 3EQ, UK
[c] William R. Wiley, Environmental Molecular Sciences Laboratory, Pacific Northwest National Laboratory, P.O. Box 999, Mail Stop K8-98 Richland, WA 99352, USA

Received 20 August 2005; revised 1 October 2005
Available online 2 November 2005

Abstract

Experimental procedures are proposed and demonstrated that separate the spectroscopic contribution from both ^{47}Ti and ^{49}Ti in solid-state nuclear magnetic resonance spectra. These take advantage of the different nuclear spin quantum numbers of these isotopes that lead to different 'effective' radiofrequency fields for the central transition nutation frequencies when these nuclei occur in sites with a significant electric field gradient. Numerical simulations and solid-state NMR experiments were performed on the TiO_2 polymorphs anatase and rutile. For anatase, the separation of the two isotopes at high field (21.1 T) facilitated accurate determination of the electric field gradient (EFG) and chemical shift anisotropy (CSA) tensors. This was accomplished by taking advantage of the quadrupolar interaction between the EFG at the titanium site and the different magnitudes of the nuclear quadrupole moments (Q) of the two isotopes. Rutile, having a larger quadrupolar coupling constant (C_Q), was examined by ^{49}Ti-selective experiments at different magnetic fields to obtain spectra with different scalings of the two anisotropic tensors. A small chemical shielding anisotropy (CSA) of −30 ppm was determined.

Keywords: QCPMG; Solid state; Isotope-selective; Ti; Multiple fields

1. Introduction

Most of the NMR active nuclei in the periodic table do not result in overlapping spectra when going to the high magnetic fields of today (i.e., up to 21.1 T). Titanium is the one exception having two NMR active isotopes, ^{47}Ti and ^{49}Ti, that exhibit almost identical Larmor frequencies and natural abundances. They differ only in their spin quantum numbers (I) and quadrupole moments (Q) [1] as displayed in Table 1. Furthermore, both Ti isotopes are low-γ (low frequency) nuclei that generally occur in sites with fairly large electric field gradients that result in significant quadrupolar coupling constants (C_Q). The result of these two factors is a significant second-order quadrupolar contribution to the linewidth of the central transition. To acquire such spectra static spin-echo type experiments [2,3] have been the most used approach because the quadrupolar coupling constant in general is too large to separate the centerband from the spinning sidebands by magic angle spinning (MAS). Single-pulse MAS or spin-echo MAS experiments have only proved successful for sites with a small/intermediate C_Q such as in $CdTiO_3$ (perovskite) and anatase [4–6]. However, the static spin-echo approach is the more generally applicable method and by this method analysis of the three polymorphs of TiO_2 [7–9], a variety of $ATiO_3$ compounds, where A was a divalent cation, a range of ternary and quaternary titanates [5,10], Ti-USY samples [11], and Ba/Sr perovskites [12] have been conducted. Some of the second-order quadrupolar broadened lineshapes originating from the central transition have been more than 100 kHz wide at 14.1 T and in order to increase

* Corresponding author. Fax: +45 35 28 32 45.
E-mail address: fhl@kvl.dk (F.H. Larsen).

1090-7807/$ - see front matter © 2005 Elsevier Inc. All rights reserved.
doi:10.1016/j.jmr.2005.10.003

Table 1
NMR parameters for ^{47}Ti and ^{49}Ti[a]

Isotope	I	Natural abundance (%)	Q (barn)	Larmor frequency at 18.8 T (MHz)
^{47}Ti	5/2	7.44	0.302	45.102
^{49}Ti	7/2	5.41	0.247	45.112

[a] Data from [1].

the S/N ratio Padro et al. [10] used the static QCPMG experiment [13–15]. Even though the sensitivity was enhanced in the ^{47,49}Ti spectrum it was noted that the central transition rf-pulses could not be optimized for both isotopes simultaneously because of different spin quantum numbers.

Previously, the QCPMG experiment has proved valuable when low-γ nuclei are of interest [16–25] and in the present work isotope-selective QCPMG experiments are presented that facilitate observation of either ^{47}Ti or ^{49}Ti lineshapes in anatase and rutile with Ti in natural abundance. We envisage that the application of this technique will also facilitate the acquisition of Ti spectra of disordered materials where two isotopic contributions can complicate spectra severely.

2. Theory

Because of their different spin quantum numbers (I) and quadrupole moments (Q) [1], the widths of the central transitions for the two isotopes are different. The relative widths of the two central transitions are given by

$$\frac{^{49}\Delta\nu_c}{^{47}\Delta\nu_c}=\frac{\left(\frac{^{49}C_Q}{8I_{49}(2I_{49}-1)}\right)^2(I_{49}(I_{49}+1)-\frac{3}{4})(^{47}\omega_0)}{\left(\frac{^{47}C_Q}{8I_{47}(2I_{47}-1)}\right)^2(I_{47}(I_{47}+1)-\frac{3}{4})(^{49}\omega_0)}=0.2843, \quad (1)$$

where $^{n}\Delta\nu_c$ denotes the width of the central transition for ^{n}Ti. The width of the central transition for ^{49}Ti is less than a third of the one from ^{47}Ti and the most well-resolved spectra will be obtained if this isotope could be selectively observed. Therefore, the primary aim is to produce spectra with lineshapes emanating from ^{49}Ti only and the secondary aim from ^{47}Ti only.

One of the differences between the two isotopes is their spin quantum number and the strategy for the isotope-selective experiments is to exploit their different flip-angles for a given rf-pulse since the effective rf-field for the central transition selective pulses is scaled by $(I+1/2)^{-1}$. By this approach the condition for observing the nucleus having spin I_1 with full intensity and not the one having spin I_2 using an echo type experiment (t_p–τ–$(2\cdot t_p)$–τ) with preparation pulse t_p may be written as

$$\begin{aligned}-\omega_{rf}t_p(I_1+1/2)&=(2k+1)\frac{\pi}{2}, \quad k\in N,\\ -\omega_{rf}t_p(I_2+1/2)&=2p\frac{\pi}{2}, \quad p\in N,\end{aligned} \quad (2)$$

where N denotes the natural numbers and $-\omega_{rf}/2\pi$ ($=\nu_{rf}$) the rf-field strength. In other words, the t_p pulse will perform as a $(\frac{\pi}{2}\pm k\pi)$-pulse on spin I_1 resulting in maximum intensity and a $(p\pi)$-pulse on spin I_2 giving zero intensity.

This leads to the condition

$$\begin{aligned}\frac{I_1+1/2}{2k+1}&=\frac{I_2+1/2}{2p}, \ p\neq 0, \ k\neq -1/2\\ \Rightarrow \quad p(2I_1+1)&=(I_2+1/2)+k(2I_2+1). \quad (3)\end{aligned}$$

That is, to observe ^{47}Ti (i.e., $I_1=5/2$) and not ^{49}Ti (i.e., $I_2=7/2$) it requires that

$$6p=4+8k\Rightarrow 3p=2+4k. \quad (4)$$

The opposite case requires that

$$8p=3+6k. \quad (5)$$

Eq. (4) has integer solutions such as $p=2$ and $k=1$ whereas Eq. (5) does not have integer solutions. This approach is, thus, not applicable to observe ^{49}Ti and in this case an addition type experiment may be used in which two echo type experiments with preparation pulses t_{p1} and t_{p2}, respectively, are added. To eliminate the ^{47}Ti signal the following conditions need to be fulfilled:

$$\left\{\begin{matrix}^{49}\text{Ti}: -4\omega_{rf}t_{p1}=\frac{\pi}{2}\\ ^{47}\text{Ti}: -3\omega_{rf}t_{p1}=\theta\end{matrix}\right\} \quad \text{and} \quad \left\{\begin{matrix}-4\omega_{rf}t_{p2}=\phi\\ -3\omega_{rf}t_{p2}=(2k+1)\pi+\theta\end{matrix}\right\}. \quad (6)$$

Consequently, the two FIDs from ^{47}Ti are going to cancel each other. The flip-angle, ϕ, of ^{49}Ti in the second spectrum also needs to be calculated to ensure that this does not annihilate the FID from the first experiment. That is, $\Delta t=t_{p2}-t_{p1}$ needs to be considered. Using this Eq. (6) is reduced to:

$$\left.\begin{matrix}\phi-\frac{\pi}{2}=-4\omega_{rf}\Delta t\\ -3\omega_{rf}\Delta t=(2k+1)\pi\end{matrix}\right\}\Rightarrow \phi-\frac{\pi}{2}=\frac{4(2k+1)\pi}{3}. \quad (7)$$

When $k=1$, the flip-angle of the second preparation pulse is increased by 4π. That is, the two ^{49}Ti FIDs of interest are added whereas the ^{47}Ti FIDs are subtracted. Another approach to suppress ^{47}Ti is adjusting the preparation pulse to an integer multiple of π for ^{47}Ti but in order to use this approach the effect on ^{49}Ti needs to be evaluated to verify that the flip-angle, ϕ, of ^{49}Ti is not an integer multiple of π as well. That is,

$$-4\omega_{rf}t_p=\phi \quad \text{and} \quad -3\omega_{rf}t_p=k\pi\Rightarrow \quad (8)$$

$$\phi=\frac{4k\pi}{3}\neq p\cdot\pi, \ \text{when } k\neq 3\cdot n, \ n\in N. \quad (9)$$

By setting $k=1$ suppression of ^{47}Ti is obtained with the shortest possible preparation pulse. In this case, $2\cdot t_p$ will not refocus the magnetization but instead ^{49}Ti-selective π pulses are used for that purpose. In summary, the proposed pulse sequences may be depicted as

$$^{47}\text{Ti}: {}^{47}\left(\frac{3\pi}{2}\right)-\tau_1-{}^{47}(3\pi)-\tau_2-\text{Acq.}\left(\frac{\tau_a}{2}\right)-[\tau_3-{}^{47}(3\pi)-\tau_4-\text{Acq.}(\tau_a)]^M-\text{Acq.}(\tau_d), \quad (10)$$

$$^{49}\mathrm{Ti}: \begin{cases} ^{49}\left(\frac{\pi}{2}\right) - \tau_1 - ^{49}(\pi) - \tau_2 - \mathrm{Acq.}\left(\frac{\tau_a}{2}\right) \\ \quad -[\tau_3 - ^{49}(\pi) - \tau_4 - \mathrm{Acq.}(\tau_a)]^M - \mathrm{Acq.}(\tau_d) \\ ^{49}\left(\frac{9\pi}{2}\right) - \tau_1 - ^{49}(9\pi) - \tau_2 - \mathrm{Acq.}\left(\frac{\tau_a}{2}\right) \\ \quad -[\tau_3 - ^{49}(9\pi) - \tau_4 - \mathrm{Acq.}(\tau_a)]^M - \mathrm{Acq.}(\tau_d) \end{cases} \tag{11}$$

or

$$^{49}\mathrm{Ti}: ^{49}\left(\frac{4\pi}{3}\right) - \tau_1 - ^{49}(\pi) - \tau_2 - \mathrm{Acq.}\left(\frac{\tau_a}{2}\right) - [\tau_3 - ^{49}(\pi) - \tau_4 - \mathrm{Acq.}(\tau_a)]^M - \mathrm{Acq.}(\tau_d) \tag{12}$$

in which $^{n}(\phi)$ denotes a selective ϕ pulse on the central transition in ^{n}Ti. The requirements for the central transition selective pulses are [26,27]

$$-\frac{2\pi C_{\mathrm{Q}}}{(4I(2I-1)\omega_{\mathrm{rf}})} > 3 \Rightarrow \tag{13}$$

$$^{47}\mathrm{Ti}: \nu_{\mathrm{rf}} < \frac{C_{\mathrm{Q}}}{120} \quad \text{and} \quad ^{49}\mathrm{Ti}: \nu_{\mathrm{rf}} < \frac{C_{\mathrm{Q}}}{252}. \tag{14}$$

The rf-field should be adjusted such that the pulses are selective for both isotopes and be as strong as possible to excite the ^{47}Ti lineshape properly.

Before performing any experiments, calculations are performed in order to validate the theoretical performance of the suggested experiments. All calculations are performed using the software described previously [15] which includes the CSA, first- and second-order quadrupolar terms as well as effects of finite rf-pulses. Furthermore, differences in natural abundance of the two isotopes are taken into account.

Two approaches for selective observation of the ^{49}Ti lineshape have been suggested. The calculated spectra produced by the pulse sequences in Eqs. (11) and (12) are displayed in Fig. 1. The spectra resulting from these two sequences in Figs. 1a and b are almost identical but the maximum intensity of the spectrum in Fig. 1a is 2.3 times the maximum intensity in Fig. 1b. As this is the sum of two FIDs the real enhancement is a factor of 1.15. Even though a possible 15% may be gained by the pulse sequence in Eq. (11) the long pulses used in the second part of pulse sequence are very likely to introduce pulse artifacts due to, e.g., rf-inhomogeneity especially for low-γ nuclei. It is therefore anticipated that this sequence will be of less practical significance and hereafter only the pulse sequence in Eq. (12) will be used for ^{49}Ti-selective spectra.

Relative to the standard QCPMG pulse sequence using ^{49}Ti central transition selective pulses depicted in Fig. 1c the two isotope-selective pulse sequences suppress the ^{47}Ti lineshape very well in the region of the ^{49}Ti lineshape and an almost pure ^{49}Ti lineshape is obtained in the central part of the spectrum. This effect is also clear when comparing the ^{47}Ti lineshapes in Figs. 1a47–c47 resulting from the three pulse sequences whereas the ^{49}Ti lineshapes seen in Figs. 1a49–c49 only display minor differences induced by the pulse sequences.

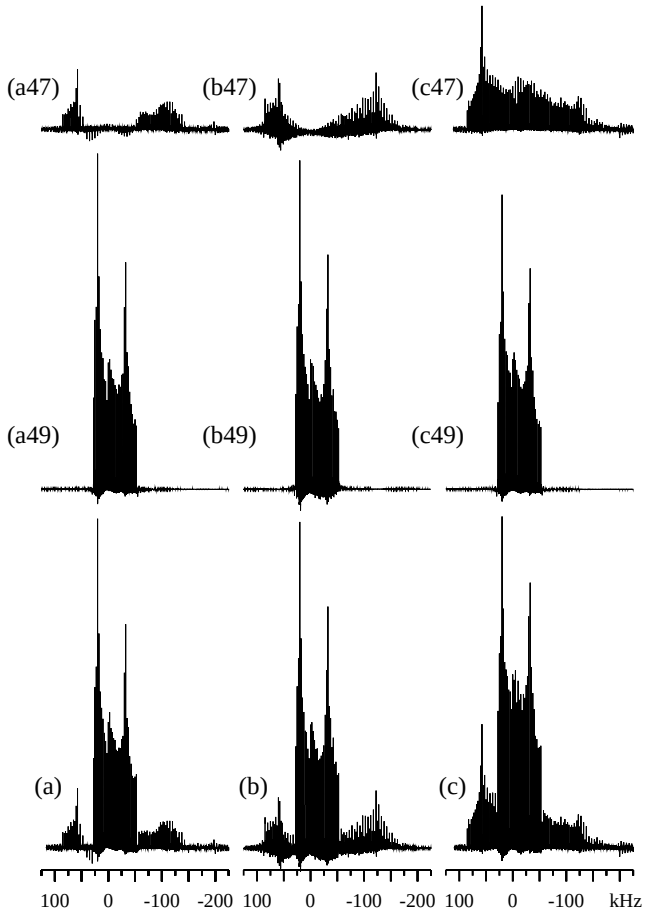

Fig. 1. Calculated ^{47}Ti,^{49}Ti spectra for a Ti site with $^{49}C_{\mathrm{Q}}$ of 15.0 MHz using the ^{49}Ti-selective pulse sequences depicted in Eq. (11) (a), Eq. (12) (b), and the standard QCPMG pulse sequence using ^{49}Ti-selective pulses (c). The Larmor frequency ($\omega_0/2\pi$) was −45.112 MHz, the rf-field strength ($-\omega_{\mathrm{rf}}/2\pi$) 40.0 kHz. All spectra are apodized by a Lorentzian linebroadening of 30 Hz. For each pulse sequence, the spectra originating from ^{47}Ti (a47,b47,c47), ^{49}Ti (a49,b49,c49), and their sum (a, b, and c) are displayed. The maximum intensity of the spectrum in (a) is 2.3 times that in (b) and the maximum intensity of the spectrum in (c) is 1.36 times that in (b).

In Fig. 2 the calculated spectra resulting from the pulse sequences in Eqs. (10) (^{47}Ti selective) and (12) (^{49}Ti selective) are presented for a Ti site having a $^{49}C_{\mathrm{Q}}$ of 15.0 MHz. The spectra are calculated at Larmor frequencies corresponding to magnetic fields of 9.4 (Figs. 2a and e), 11.7 (Figs. 2b and f), 14.1 (Figs. 2c and g), and 18.8 T (Figs. 2d and h), respectively. In the calculated ^{47}Ti-selective spectra (Figs. 2a–d), a good suppression of the lineshape originating from ^{49}Ti is observed at all magnetic field strengths. At lower magnetic field strengths (Figs. 2a and b) the effects of finite rf-pulses are very pronounced and only at 14.1 and 18.8 T (Figs. 2c and d) both singularities in the ^{47}Ti lineshape are observed but even at these high fields effects of finite rf-pulses are clearly present. This illustrates that high fields are required if

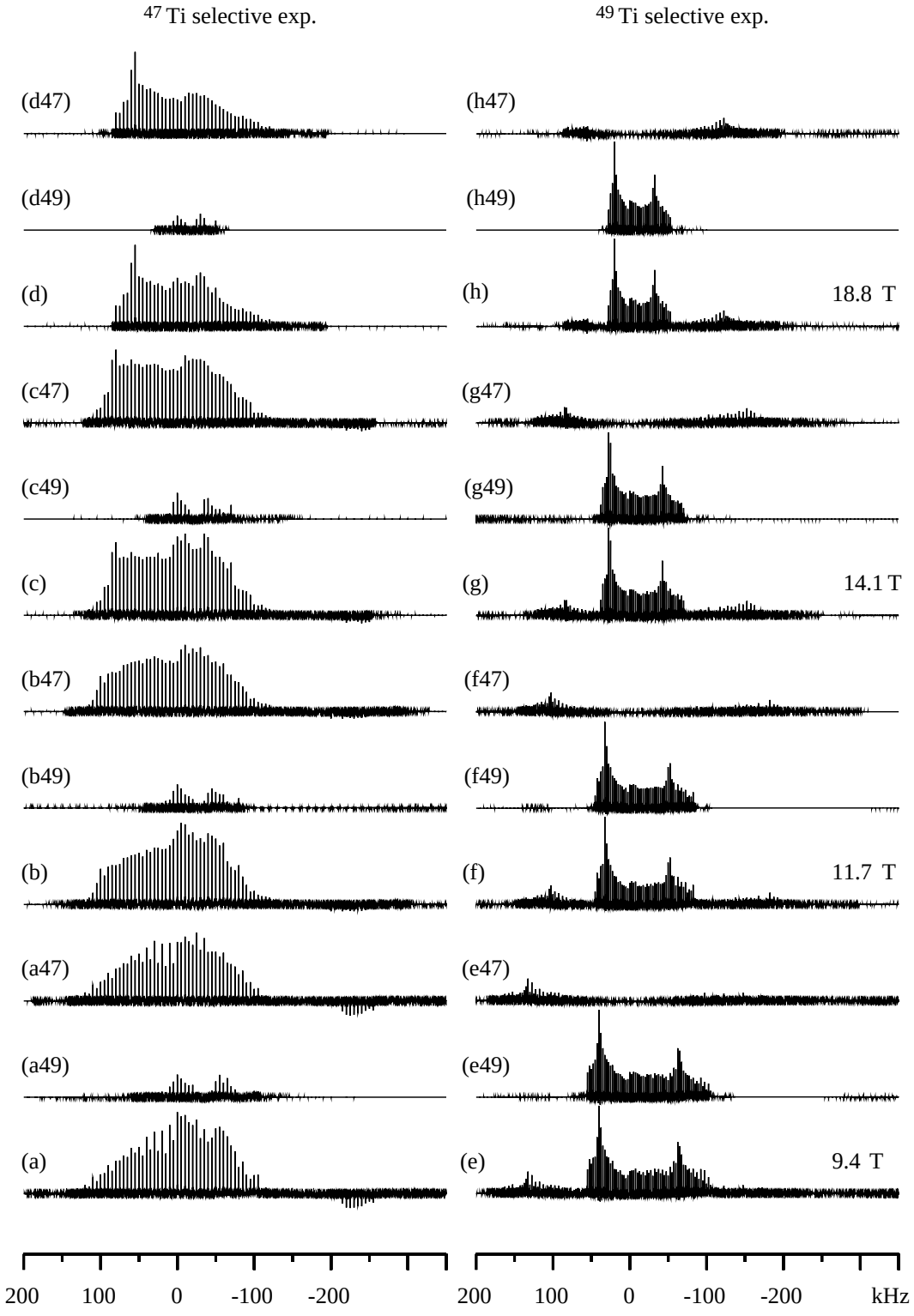

Fig. 2. Calculated ^{47}Ti,^{49}Ti spectra for at Ti site with $^{49}C_Q$ of 15.0 MHz using the ^{47}Ti-selective pulse sequence depicted in Eq. (10) (a–d) and the ^{49}Ti-selective pulse sequence in Eq. (12) (e–h). The Larmor frequencies ($\omega_0/2\pi$) were −22.53 MHz (a and e), −28.16 MHz (b and f), −33.80 MHz (c and g), and −45.06 MHz (d and h), respectively. The spectra in (a–d) employed a rf-field strength ($-\omega_{rf}/2\pi$) of 60.0 kHz whereas the spectra in (e–h) were calculated using a rf-field strength ($-\omega_{rf}/2\pi$) of 50.0 kHz. All spectra are apodized by a Lorentzian linebroadening of 50 Hz. For each Larmor frequency, the spectrum originating from ^{47}Ti (a47–h47), ^{49}Ti (a49–h49), and their sum (a–h) is displayed.

the ^{47}Ti-selective pulse sequence in Eq. (10) is going to be applied for analysis of Ti sites with large quadrupolar couplings.

The spectra in Figs. 2e47–h47 in the right column of Fig. 2 display a good suppression of the ^{47}Ti lineshape at all magnetic fields. The suppression of ^{47}Ti is especially

good in the region of the ^{49}Ti lineshape close to proximity of the rf transmitter frequency. At every magnetic field strength a well-defined second-order lineshape is observed for ^{49}Ti with no significant distortion due to finite rf-pulses, which makes this experiment very well suited for analysis of Ti sites with large $^{49}C_Q$'s even at intermediate magnetic field strengths (i.e., 9.4 and 11.7 T).

In Fig. 3 calculated spectra similar to those in Fig. 2, but with a Ti site having $^{49}C_Q$ of 5.0 MHz, are displayed. In this case, both isotope-selective experiments perform well at all magnetic field strengths with no significant distortions in the spectra introduced by of finite rf-pulses.

When selective experiments of both isotopes can be successfully performed at the same magnetic field strength, two spectra with different scaling of the EFG-tensor are obtained. This points to more accurate determination of the quadrupolar and in particular the CSA-tensor using only

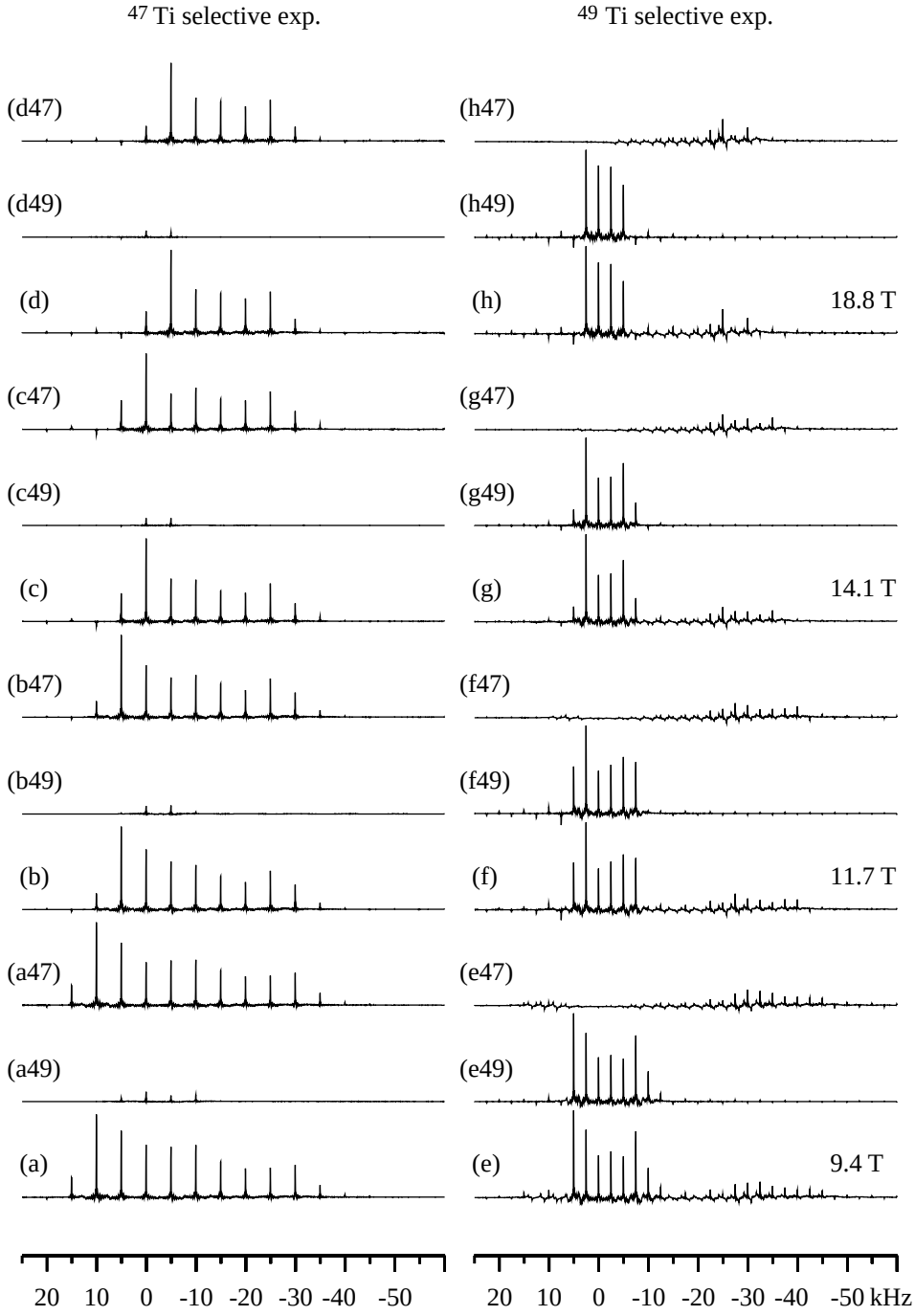

Fig. 3. Calculated ^{47}Ti,^{49}Ti spectra for a Ti site with a $^{49}C_Q$ of 5.0 MHz. Parameters were identical to the one in the caption of Fig. 2 besides the rf-field strength ($-\omega_{rf}/2\pi$) that was 20.0 kHz for the spectra in (a–d) and 15.625 kHz for the spectra in (e–h).

one magnetic field for Ti sites with small and intermediate $^{49}C_Q$'s.

3. Experimental

The ^{47}Ti and ^{49}Ti NMR spectra were recorded at ambient temperature using a wide-bore Varian Unity Plus 500 (11.7 T) spectrometer operating at 28.207 MHz equipped with a 5 mm static-powder probe from Doty Scientific, medium-bore Varian Inova 800 (18.8 T) spectrometer operating at 45.100 MHz using a homebuilt 5 mm static-powder probe, and a medium-bore Varian Inova 900 (21.1 T) spectrometer operating at 50.754 MHz using a homebuilt 5 mm static-powder probe. At all magnetic fields, the rf-powers were adjusted to be well within the selective pulse regime. The ^{47,49}Ti NMR spectra were referenced to the ^{49}Ti resonance in neat liquid $TiCl_4$ unless stated otherwise.

Spectral simulations and iterative fitting were performed using the program described elsewhere [15] taking effects of finite rf-pulses into account. All spectral simulations employed η_Q of 0.25, $\delta_{iso} = 0.0$ ppm, $\tau_i = 100$ μs ($i = 1, \ldots, 4$), $\tau_d = 250$ μs, and a dwell time of 0.5 μs. The simulations for the ^{49}Ti-selective experiments (Eqs. (11) and (12)) employed $M = 25$ and $\tau_a = 400$ μs, whereas $M = 50$ and $\tau_a = 200$ μs were used for the ^{47}Ti-selective experiment (Eq. (10)). The transmitter was set to 0 ppm (on-resonance) for the nucleus of interest in the simulated isotope-selective experiments.

The sample of anatase was obtained from Aldrich (Cat. No. 23,203-3) whereas the rutile sample was an X-ray standard from Standard Reference Material 674, National Bureau of Standards.

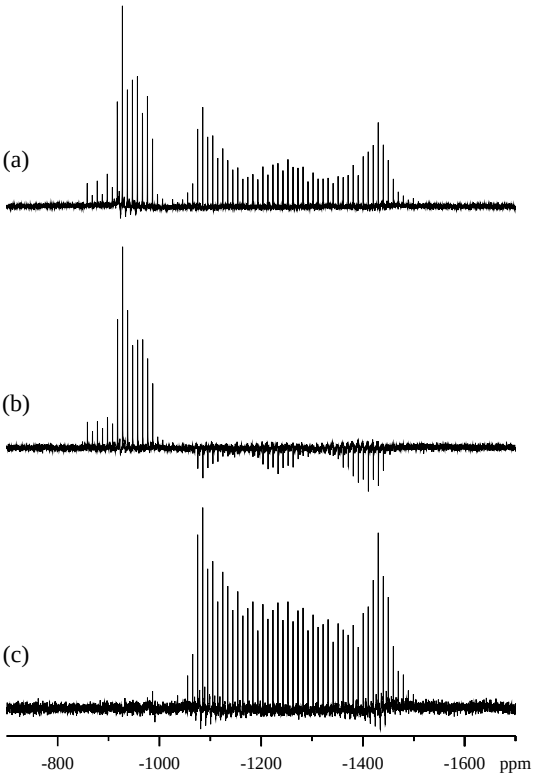

Fig. 4. Experimental ^{47}Ti,^{49}Ti spectra of anatase acquired at 21.1 T (50.75 MHz) (a–c) using the QCPMG pulse sequence with ^{49}Ti-selective pulses (a), the ^{49}Ti-selective pulse sequence in Eq. (12) (b) and the ^{47}Ti-selective pulse sequence in Eq. (10) (c). All experiments employed an rf-field strength of 12.5 kHz, $\tau_1 = 50.0$ μs, $\tau_2 = \tau_4 = 76.0$ μs, and $\tau_3 = 24.0$, $M = 50$, $\tau_a = 2.0$ ms, a dwell time of 2.0 μs, and 512 scans. All experiments were acquired using a recycle delay of 5 s and apodized by Lorentzian linebroadening of 10 Hz.

4. Results and discussion

Fig. 4 shows the experimental spectra of anatase using the QCPMG pulse sequence with ^{49}Ti-selective pulses (Fig. 4a), the ^{49}Ti-selective pulse sequence in Eq. (12) (Fig. 4b), and the ^{47}Ti-selective pulse sequence in Eq. (10) (Fig. 4c) acquired at 21.1 T. An almost perfect separation of the lineshapes of the two isotopes is obtained using the isotope-selective pulse sequences. In the ^{49}Ti-selective spectrum (Fig. 4b), some of the ^{47}Ti lineshape is observed with low negative intensity and in the ^{47}Ti-selective spectrum (Fig. 4c) the remains of the ^{49}Ti lineshape are barely visible. Due to larger quadrupole moment and lower spin quantum number, the effect of the second-order quadrupolar broadening is greater for ^{47}Ti than for ^{49}Ti and this interaction is most prominent in the ^{47}Ti subspectrum. The CSA on the other hand remains the same for both isotopes but the effect is most clearly seen in the ^{49}Ti subspectrum because of the smaller second-order quadrupolar broadening. In the context of determination of CSA- and EFG-parameters, this allows for extraction of accurate parameters using both isotopically selective spectra obtained at one magnetic field and avoids acquisition of spectra at different magnetic fields to observe the different field dependence of the two anisotropic interactions. This strategy was used for simultaneous iterative fitting of the isotope-selective anatase spectra in Figs. 4b and c. As can be seen in Fig. 5, a good agreement between the experimental (Figs. 5a and c) and calculated (Figs. 5b and d) spectra was obtained using the parameters in Table 2. The calculated spectra of the individual isotopes are displayed below the total calculated spectra (Figs. 5b49, b47, d49, and d47). To illustrate that the chemical shift is independent of which isotope is analyzed, the ^{47}Ti-selective spectra (Figs. 5a, b, b49, and b47) are referenced to the ^{47}Ti resonance in $TiCl_4$(l).

The isotropic chemical shift and magnitude of the EFG-parameters ($^{49}C_Q$, η_Q) obtained for anatase are similar to the values obtained previously [4,8,6] except for δ_{iso} at −1038 ppm determined by Bastow et al. [8] that is significantly different from the others. Regarding the CSA, the magnitude of δ_σ in our study is 18 ppm larger than the one determined by Brãuniger et al. [6] but agrees very well with the values obtained by single-crystal NMR [29]. This underlines the importance of the highest possible magnetic field when accurate determination of smaller anisotropic interactions is of interest.

For intermediate or small $^{49}C_Q$'s the approach described above is easily applicable but for larger anisotropic

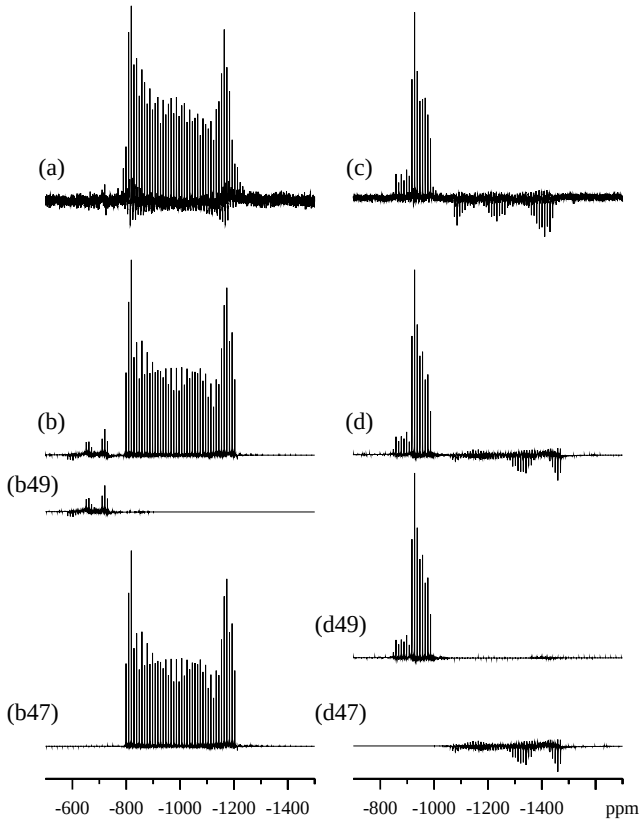

Fig. 5. Experimental (a and c) and calculated (b and d) spectra of anatase at 21.1 T (50.75 MHz) using the ^{47}Ti-selective pulse sequence (Eq. (10)) (a and b) and the ^{49}Ti-selective pulse sequence (Eq. (12)) (c and d), respectively. The spectra are calculated using the parameters listed in Table 2. Both experimental and calculated spectra employ the experimental conditions listed in the caption of Fig. 4. The calculated spectra for both isotopes (b and d) are sums of the contributions from ^{49}Ti (b49,d49) and ^{47}Ti (b47,d47), respectively. All calculated spectra were apodized by Lorentzian linebroadenings of 10 Hz. The spectra in (a) and (b, b49, and b49) are referenced relative to the ^{47}Ti resonance in $TiCl_4$ (l).

interactions it is difficult experimentally to excite the broad lineshapes corresponding to the ^{47}Ti isotope as expected from the calculated spectra in Fig. 2. For instance, limited bandwidth of the probe or pulse artifacts may become important factors and introduce effects that are very difficult to compensate for. Therefore, rutile has been examined by the ^{49}Ti-selective pulse sequence in Eq. (12) at 11.7, 18.8, and 21.1 T in order to accurately determine anisotropic parameters. In Fig. 6, experimental (Figs. 6a, c, and e) and calculated (Figs. 6b, d, and f) spectra are displayed. Shown below each calculated spectrum are the contributions from the ^{49}Ti (Figs. 6a49–e49) and ^{47}Ti (Figs. 6a47–e47) isotopes. The parameters in Table 2 were employed for the calculated spectra. The EFG-parameters are almost identical to the ones determined by single-crystal NMR performed at 4.2 and 8.5 T [28] and the high field spectra even allowed for determination of a small δ_σ of -30 ± 15 ppm which is in accordance with the value of -47 ± 20 ppm determined by a more recent single-crystal NMR study carried out at 11.7 T [29]. The isotropic chemical shift of -881 ppm is similar to the value of -860 ppm determined by single-crystal NMR [29] and less than 40 ppm off the values determined from a powder spectrum at 9.4 T [8]. Overall, a good fit was obtained at all fields, but particularly at 11.7 T the intensity of the ^{47}Ti lineshape is difficult to calculate accurately due to the experimental conditions previously mentioned.

5. Conclusions

The NMR lineshapes of the two Ti isotopes can be separated by isotope-selective ^{47}Ti/^{49}Ti QCPMG type experiments. The ^{49}Ti-selective pulse sequence is the method of choice for both small and large quadrupole coupling constants at high and intermediate magnetic field strengths. The ^{47}Ti-selective pulse sequence, that can provide

Table 2
Quadrupole coupling (C_Q, η_Q), isotropic and anisotropic chemical shift ($\delta_{iso}, \delta_\sigma, \eta_\sigma$) parameters determined by iterative fitting of ^{47,49}Ti QCPMG powder spectra in natural abundance[a]

Compound	C_Q (MHz)	η_Q	δ_{iso} (ppm)[b]	δ_σ (ppm)	η_σ	Ω_σ^{PC}[e]	Reference
Anatase	4.94 ± 0.05	0.06 ± 0.02	-927 ± 2	-78 ± 4	0.10 ± 0.05	(254,179,97)	Figs. 5b and f
	4.6	0.0	−916[c], −920[d]				[4]
	4.79	0	−1038				[8]
	4.85 ± 0.10	0.0[f]	-920 ± 15	−80	0.0[f]	(0,0,0)	[29]
	4.9	0.0	−912	60			[6]
Rutile	13.91 ± 0.10	0.20 ± 0.02	-881 ± 5	-30 ± 15	1.0	(80,110,81)	Figs. 6b, f, and j
	13.9	0.19					[28]
	13.9[g]	0.19[g]	−843				[8]
	13.9[g]	0.19[g]	-860 ± 10	-47 ± 20	0.0	(0,0,0)	[29]

[a] Accuracies are estimated by numerical calculations and visual inspection.
[b] Referenced to neat liquid $TiCl_4$.
[c] 11.7 T.
[d] 14.1 T.
[e] Accuracies are ±20 for the angles.
[f] Fixed value.
[g] Parameter fixed at the values found by Kanert et al. [28].

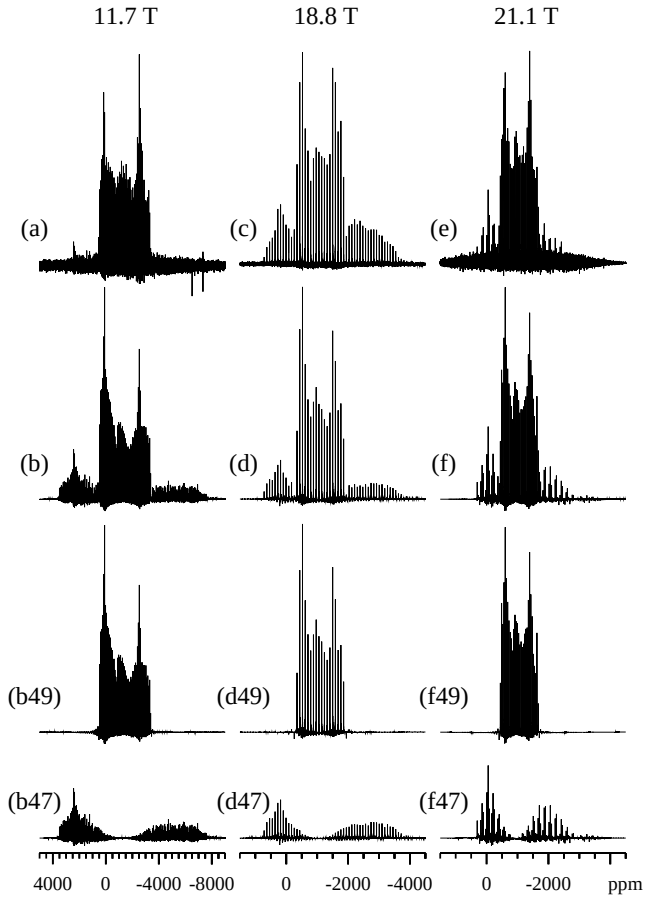

Fig. 6. Experimental (a, c, and e) and calculated (b, d, and f) spectra of rutile at 11.7 (a, b), 18.8 (c, d), and 21.1 T (e, f) using the ^{49}Ti-selective pulse sequence in Eq. (12). The parameters listed in Table 2 are used for the calculated spectra. These also employed the experimental conditions for the experimental spectra which were: (a) an rf-field strength of 41.7 kHz, $\tau_1 = 150.0$ μs, $\tau_2 = \tau_4 = 154.5$ μs, and $\tau_3 = 145.5$, $M = 50$, $\tau_a = 500$ μs, a dwell time of 1.0 μs, 32,768 scans with a recycle delay of 5 s and apodization by Lorentzian linebroadening of 10 Hz, (c) an rf-field strength of 27.8 kHz, $\tau_1 = 80.0$ μs, $\tau_2 = \tau_4 = 83.6$ μs, and $\tau_3 = 76.4$, $M = 100$, $\tau_a = 250$ μs, a dwell time of 1.0 μs, 8192 scans with a recycle delay of 2.5 s and apodization by Lorentzian linebroadening of 15 Hz, (e) an rf-field strength of 19.2 kHz, $\tau_1 = 50.0$ μs, $\tau_2 = \tau_4 = 55.0$ μs, and $\tau_3 = 45.0$, M = 100, $\tau_a = 500$ μs, a dwell time of 1.0 μs, 512 scans with a recycle delay of 5 s and apodization by Lorentzian linebroadening of 10 Hz. The calculated spectra for both isotopes (b, d, and f) are sums of the contributions from ^{49}Ti (b49,d49,f49) and ^{47}Ti (b47,d47,f47), respectively. All calculated spectra were apodized by Lorentzian linebroadenings of 15 Hz.

additional information on the CSA, is only useful for small or intermediate C_Q's with currently available magnetic field strengths. However, compared with the ^{49}Ti-selective pulse sequence the ^{47}Ti-selective pulse sequence provides a more efficient suppression of the unwanted lineshape. By iterative fitting, isotropic and anisotropic parameters have been determined for rutile and anatase based on either selective spectra of both isotopes at one magnetic field strength or ^{49}Ti-selective spectra at multiple fields.

It is foreseen that these experiments will be of great significance for future Ti NMR projects as spectral separation of the two isotopes simplifies spectra of compounds with multiple Ti sites and therefore makes Ti NMR a more generally applicable analytical tool.

Acknowledgment

The experimental part of this research was performed in the Environmental Molecular Sciences Laboratory (a national scientific user facility sponsored by the U.S. DOE Office of Biological and Environmental Research) located at Pacific Northwest National Laboratory, operated by Batelle for the DOE.

References

[1] R.K. Harris, E.D. Becker, NMR nomenclature: nuclear spin properties and conventions of chemical shifts—IUPAC recommendations, J. Magn. Reson. 156 (2002) 323–326.
[2] E.L. Hahn, Spin echoes, Phys. Rev. 80 (1950) 580–594.
[3] I. Solomon, Multiple echoes in solids, Phys. Rev. 110 (1958) 61–65.
[4] S.F. Dec, M.F. Davis, G.E. Maciel, C.E. Bronnimann, J.J. Fitzgerald, S. Han, Solid-state multinuclear NMR studies of ferroelectric, piezoelectric, and related materials, Inorg. Chem. 32 (1993) 955–959.
[5] D. Padro, A.P. Howes, M.E. Smith, R. Dupree, Determination of titanium NMR parameters of $ATiO_3$ compounds: correlation with structural distortion, Solid State Nucl. Magn. Reson. 15 (2000) 231–236.
[6] T. Bräuniger, P.K. Madhu, A. Pampel, D. Reichert, Application of fast amplitude-modulated pulse trains for signal enhancement in static and magic-angle-spinning ^{47,49}Ti-NMR spectra, Solid State Nucl. Magn. Reson. 26 (2004) 114–120.
[7] A. Labouriau, W.L. Earl, Titanium solid-state NMR in anatase, brookite and rutile, Chem. Phys. Lett. 270 (1997) 278–284.
[8] T.J. Bastow, M.A. Gibson, C.T. Forwood, ^{47,49}Ti NMR: hyperfine interactions in oxides and metals, Solid State Nucl. Magn. Reson. 12 (1998) 201–209.
[9] T.J. Bastow, G. Doran, H.J. Whitfield, Electron diffraction and ^{47,49}Ti and ^{17}O NMR studies of natural and synthetic brookite, Chem. Mater. 12 (2000) 436–439.
[10] D. Padro, V. Jennings, M.E. Smith, R. Hoppe, P.A. Thomas, R. Dupree, Variations of titanium interactions in solid state NMR-correlations to local structure, J. Phys. Chem. B 106 (2002) 13176–13185.
[11] S. Ganapathy, K.U. Gore, R. Kumar, J.-P. Amoureux, Multinuclear (^{27}Al, ^{29}Si, ^{47,49}Ti) solid-state NMR of titanium substituted zeolite USY, Solid State Nucl. Magn. Reson. 24 (2003) 184–195.
[12] C. Gervais, D. Veautier, M.E. Smith, F. Babonneau, P. Belleville, C. Sanchez, Solid state ^{47,49}Ti, ^{87}Sr and ^{137}Ba NMR characterisation of mixed barium/strontium titanate perovskites, Solid State Nucl. Magn. Reson. 26 (2004) 147–152.
[13] H.Y. Carr, E.M. Purcell, Effects of diffusion on free precession in nuclear magnetic resonance experiments, Phys. Rev. 94 (1954) 630–638.
[14] S. Meiboom, D. Gill, Modified spin-echo method for measuring nuclear relaxation times, Rev. Sci. Instrum. 29 (1958) 688–691.
[15] F.H. Larsen, H.J. Jakobsen, P.D. Ellis, N.C. Nielsen, Sensitivity-enhanced quadrupolar-echo NMR of half-integer quadrupolar nuclei. Magnitudes and relative orientation of chemical shielding and quadrupolar coupling tensors, J. Phys. Chem. A 101 (1997) 8597–8606.
[16] F.H. Larsen, A.S. Lipton, H.J. Jakobsen, N.C. Nielsen, P.D. Ellis, ^{67}Zn QCPMG solid-state NMR studies of zinc complexes as models for metalloproteins, J. Am. Chem. Soc. 121 (1999) 3783–3784.
[17] F.H. Larsen, J. Skibsted, H.J. Jakobsen, N.C. Nielsen, Solid-state QCPMG NMR of low-γ quadrupolar metal nuclei in natural abundance, J. Am. Chem. Soc. 122 (2000) 7080–7086.

[18] A.S. Lipton, G.W. Buchko, J.A. Sears, M.A. Kennedy, P.D. Ellis, ^{67}Zn solid-state NMR spectroscopy of the minimal DNA binding domain of human nucleotide excision repair protein XPA, J. Am. Chem. Soc. 123 (2001) 992–993.

[19] A.S. Lipton, J.A. Sears, P.D. Ellis, A general strategy for the NMR observation of half-integer quadrupolar nuclei in dilute environments, J. Magn. Reson. 151 (2001) 48–59.

[20] I. Hung, R.W. Schurko, Solid-state ^{25}Mg QCPMG NMR of bis(cyclopentadienyl)magnesium, Solid State Nucl. Magn. Reson. 24 (2003) 78–93.

[21] R.W. Schurko, I. Hung, C.M. Widdifield, Signal enhancement in NMR spectra of half-integer quadrupolar nuclei via DFS-QCPMG and RAPT-QCPMG pulse sequences, Chem. Phys. Lett. 379 (2003) 1–10.

[22] I. Hung, R.W. Schurko, Solid-State ^{91}Zr NMR of Bis(cyclopentadienyl)dichlorozirconium(IV), J. Phys. Chem. B 108 (2004) 9060–9069.

[23] K.J. Ooms, R.E. Wasylishen, Solid-state Ru-99 NMR spectroscopy: a useful tool for characterizing prototypal diamagnetic ruthenium compounds, J. Am. Chem. Soc. 126 (2004) 10972–10980.

[24] A. Wong, R.D. Whitehead, Z. Gan, G. Wu, A solid-state NMR and computational study of sodium and potassium tetraphenylborates: ^{23}Na and ^{39}K NMR signatures for systems containing cation-π interactions, J. Phys. Chem. A 108 (2004) 10551–10559.

[25] C.M. Widdifield, R.W. Schurko, A solid-state ^{39}K and ^{13}C NMR study of polymeric potassium metallocenes, J. Phys. Chem. A 109 (2005) 6865–6876.

[26] A. Abragam, Principles of Nuclear Magnetism, Oxford University Press, Oxford, 1961.

[27] N.C. Nielsen, H. Bildsøe, H.J. Jakobsen, Finite rf pulse excitation in MAS NMR of quadrupolar nuclei. Quantitative aspects and multiple-quantum excitation, Chem. Phys. Lett. 191 (1992) 205–212.

[28] O. Kanert, H. Kolem, The unusual temperature dependence of the electric field gradient at titanium sites in rutile (TiO_2), J. Phys. C 21 (1988) 3909–3916.

[29] L.V. Dmitrieva, L.S. Vorotilova, I.S. Podkorytov, M.E. Shelyapina, A comparison of NMR spectral parameters of ^{47}Ti and ^{49}Ti nuclei in anatase and rutile, Phys. Solid State 41 (1999) 1097–1099.